Resource Operators Conference

Faculty of Engineering and Information Sciences

2021

Dynamic model of fault slip and its effect on coal bursts in deep mines

Jan Nemcik
University of Wolllongong

Gaetano Venticinque
SCT Operations Pty Ltd

Zhenjun Shan
University of Wollongong

Libin Gong
Institute of Geonics, the Czech Academy of Sciences

Recommended Citation

Jan Nemcik, Gaetano Venticinque, Zhenjun Shan, and Libin Gong, Dynamic model of fault slip and its effect on coal bursts in deep mines, in Naj Aziz and Bob Kininmonth (eds.), Proceedings of the 2021 Resource Operators Conference, Mining Engineering, University of Wollongong, 18-20 February 2019
https://ro.uow.edu.au/coal/808

DYNAMIC MODEL OF FAULT SLIP AND ITS EFFECT ON COAL BURSTS IN DEEP MINES

Jan Nemcik[1], Gaetano Venticinque[2], Zhenjun Shan[1] and Libin Gong[3]

ABSTRACT: The success of deep mining operations relies upon controlling the fractured ground. It is a documented knowledge that many coal bursts occur when mining close to the existing faults. Gradual stress relief towards excavations and other mechanisms can unload stress normal to the nearby fault plane causing it to slip. The generated seismic waves impact the mine roadway rib sides and can produce a coal burst. As part of the ACARP project, the $FLAC^{3D}$ dynamic numerical model was used to show how a fault slip at various locations and orientations may initiate a coal burst. This study simulates an artificial fault slip with peak velocity reaching 4m/s in 0.013 seconds and displacing 119mm in total. Seismic induced peak particle velocities in rock and its influence on coal rib stability were investigated. 89 numerical models with various fault locations and orientations at 450m depth indicated that a 4 tonne coal block can be ejected from the mine roadway rib side at speeds of up to 5m/s. The important finding is that irrespective of the fault slip magnitude, the fault geometry and the in-situ stresses enable to predict which side of the mine roadway may experience the coal burst. Instructing the mine personnel to use the other side of the roadway may improve their safety. Overall, this research produced preliminary results to prove that this method can be used to flag the coal burst dangers for certain fault locations and orientations in deeper mines irrespective of the fault slip properties that are typically difficult to predict.

INTRODUCTION

Historical data indicate that in deep mines presence of faults in close proximity to excavations affect the frequency of coal bursts. An extensive work by many researchers has attempted to correlate the fault geometry and its orientation on severity of coal bursts. For example, White and Whyatt (1999a,b) investigated the mechanism of rockbursts that took place at the Lucky Friday Mine in the USA reporting that slip movements of a steeply dipping fault towards a nearby stope resulted in an increased compressive stress near the stope, which contributed to the occurrence of rockbursts experienced. Blake and Hedley(2003), Ortlepp,(2000) and others studied peak particle velocities within rock induced by seismic waves, causing severe ground motions and damage to the rock mass.

To date, no comprehensive dynamic modelling has been attempted to show the direct mechanism of how the fault slip affects both coal rib ejection magnitude and location in the mine roadway. The preliminary dynamic models of Nemcik and Venticinque (2019) attempted to show how fault slips at various orientations may affect the coal bursts.

3-DIMENSIONAL DYNAMIC ANALYSIS OF FAULT SLIPS AND THEIR INFLUENCE ON COAL RIB STABILITY

Numerous models with various fault locations and orientations were constructed adjacent to the coal mine roadway. An identical fault slip of a fixed magnitude was modelled for these geometries to enable comparison between rib ejection magnitudes and directions. To evaluate the influence of fault slip on coal rib stability, an average ejection energy at the rib side was calculated for 1m length of roadway from the kinetic momentum of an ejected 4 tonne coal block attached to the rib side. This study was aimed at producing preliminary results to prove that this method can be used to flag the coal burst dangers for certain fault orientations and excavation localities. To avoid any complications that may arise due to yield zones, elastic models were set up to carry out a number of sensitivity studies. The fault orientation, its distance from the excavation and fault slip direction were studied to estimate the severity of coal burst and side of the roadway that the coal burst may occur.

1 Faculty of Engineering and Information Sciences, University of Wollongong
2 SCT Operations Pty LTD, Australia
3 Researcher, Institute of Geonics, the Czech Academy of Sciences

FLAC3D Dynamic Model Setup

The constructed model was 80m wide (perpendicular to the mined roadway), 80m high (in vertical direction) and 40m thick (in excavation direction) as shown in Figure 1. Examining combinations of different fault geometries, the first 44 modelled instances were characterised with a fault plane aligned against the excavation of a 5m wide mine roadway running entirely through the centre of a 3m thick coal seam. A 'continuous' 2.9 m high and 1m thick coal block was attached to the rib side in the mine roadway to measure its kinetic momentum due to seismic waves. For the remaining 45 fault models a shorter mine roadway was excavated to the centre of the model and a 1m thick, 2.9m high and 2m long coal block was attached to the rib side adjacent to the roadway face. Elastic properties of the strata were chosen to enable measurements of the maximum possible kinetic energy transfer through the rock or coal seam without complications of the yielded zones. Typical sandstone rock and coal properties were assigned to the roof, floor and the coal seam as specified in Table 1.

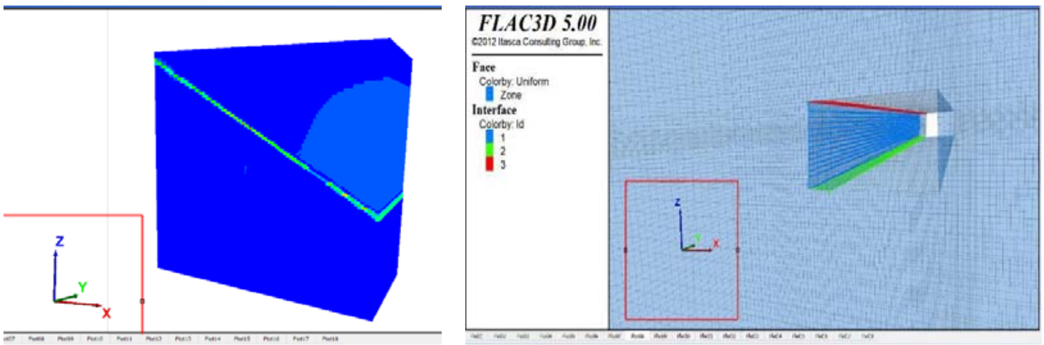

Figure 1 Model geometry showing one of the slipping faults and the mine roadway

Table 1 Model Strata Properties

Strata type	Density (kg/m^3)	Bulk Modulus (GPa)	Shear Modulus (GPa)
Roof and Floor Sandstone	2500	10.67	6.4
Coal Seam	1400	3.33	1.11

The models were initially run until static equilibrium was achieved. A simple one-way dynamic fault slip was then artificially modelled by assigning variable slip velocities along the fault using the following decay equation:

$$y(t) = A^{-\lambda ct}\cos(2\pi ct + \varphi)$$

Where *A=Wave amplitude (18.4 m/s – not the actual velocity produced),* λ *is a Constant=10,* φ *is Phase=90°,* c *is a Constant=7 and* t*=Time (between 0 to 0.07s)*

The equation constants were chosen to produce a maximum slip velocity (V_p) of 4 m/s incipient at time t=0.013 seconds and subsequently decaying to zero at approximately 0.07 seconds producing an overall maximum displacement of 119mm along the dip of the fault. Note that for the sensitivity studies the artificial fault slip was preferred as the 'modelled slip may have produced variable results due to the model boundaries and other constrains. The V_p value adopted here from (pulse like rupture) is only an estimate based on previous Earthquake research data (Bizzari, 2012).

Assigned to the wave function in FLAC^{3D} dynamic model FISH subroutine, this wave command produced maximum fault slip velocity of 4 m/s 0.013 seconds after the slip began (Figure 2) with seismic waves spreading through the surrounding strata at sonic speeds.

It may be confusing to think of seismic waves as 'extremely fast compressive or shear fronts' travelling at several km/s. It seems instead more logical to rather interpret the movement of the rock matrix by considering the 'rock particles' themselves and their maximum velocities (as vectors) also known as peak particle velocities (*PPV*) which occur at some many orders of magnitude slower (ie several m/s) with potential to disturb the unconfined rock/coal at the boundaries The conservation of kinetic momentum for a seismic wave can also be better understood by imagining the 'small rock particle collisions' within the wave front to follow a similar momentum transfer as the balls in Newton's famous cradle experiment.

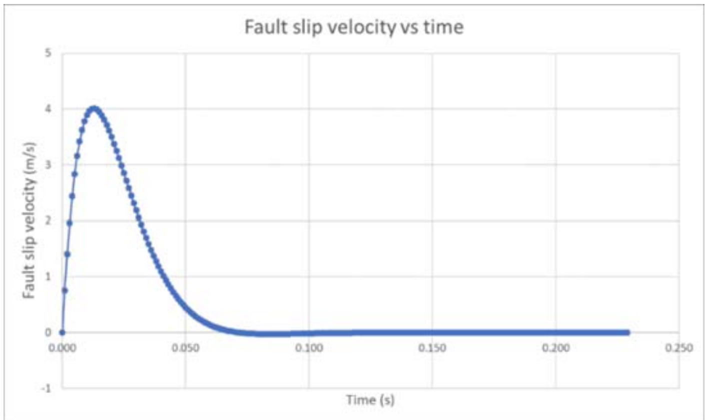

Figure 2 Fault slip velocity versus time

Modelled Fault Slip at Various Fault Orientations and their Influence on Rib Stability in Mine Roadway

Fault slips along planar faults orientated at various locations and inclinations were trialled over 44 modelled instances to quantify the values of the energy imparted on the coal rib side.

Horizontal faults parallel to the seam were modelled at locations 2m, 5m, 10m, 15m, 20m and 30m below the seam floor which was also repeated for above the seam roof. These faults were subsequently rotated from 0° to dips of 15°, 30°, 45°, and 60° through the fault rotation point which was located below and above the roadway centre depending on fault location. An additional 45 runs of the vertical fault at various distance and bearings ahead of the roadway face were also trialled.

These fault slips were also arranged such that imparting seismic velocities produced by the slip travelled in a direction towards the rib side having the attached 1 m wide coal block. The attached block attempted to emulate the yielded and low confined state of the coal mass typically found in the rib. As the fault slipped, seismic waves carried the kinetic energy (momentum) towards the rib, imparting into the block and ejecting it from the rib side. This mechanism provided a controlled means of measuring impact velocities of the seam particles generated by the seismic waves at the coal rib. Figure 3a and 3b aid to assist with visualision of the model's geometry and how block ejection velocities were recorded. After dissipation of the seismic waves through the surrounding strata, seismic momentum accumulated within the block remain locked inside propelling it to velocities above 4 m/s.

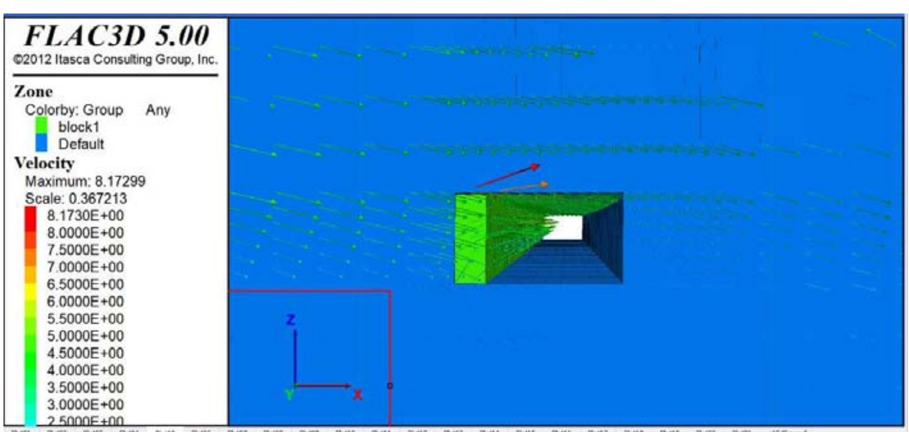

Figure 3a Development of velocities induced by nearby slipping fault (15° dip) 5m above the roadway at time of 0.012 seconds after fault slip began.

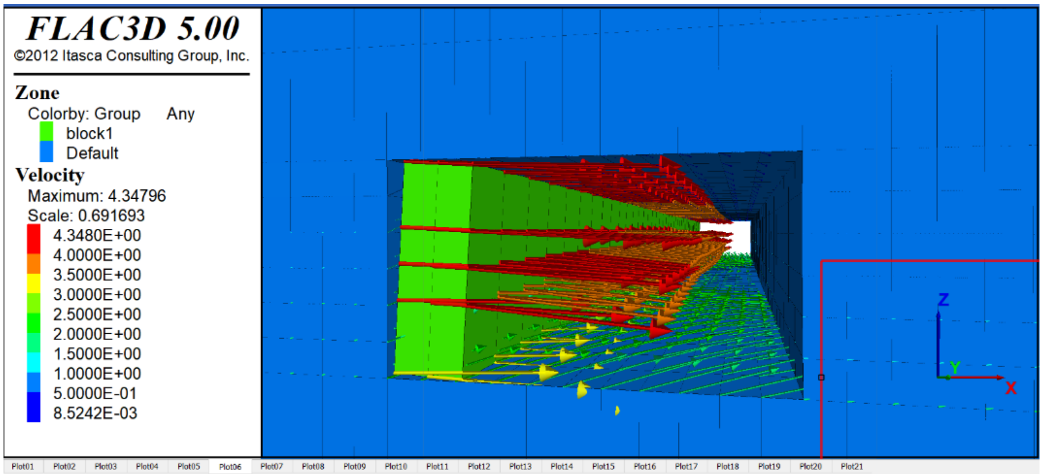

Figure 3b View inside of the excavated mine roadway showing the 'same coal block' ejection away from the rib side at an average velocity above 4 m/s at time of 0.07 seconds after slip begun

Calculations of coal block ejection velocities, momentum and energy were performed for each instance of the 44 modelled faults having various inclinations parallel to the mine roadway and are summarised in Table 2.

For the vertical fault models (those numbered 45 to 89) the mine roadway was excavated half way (i.e. to the centre of the model) and faults inserted in front of the roadway face. A coal block 1m thick 2.9m high and 2m long was attached to the roadway rib side adjacent to the roadway face as shown in Figure 4. After the seismic waves dissipated, the momentum locked inside the block propelled the block at typical velocities of approximately 4m/s.

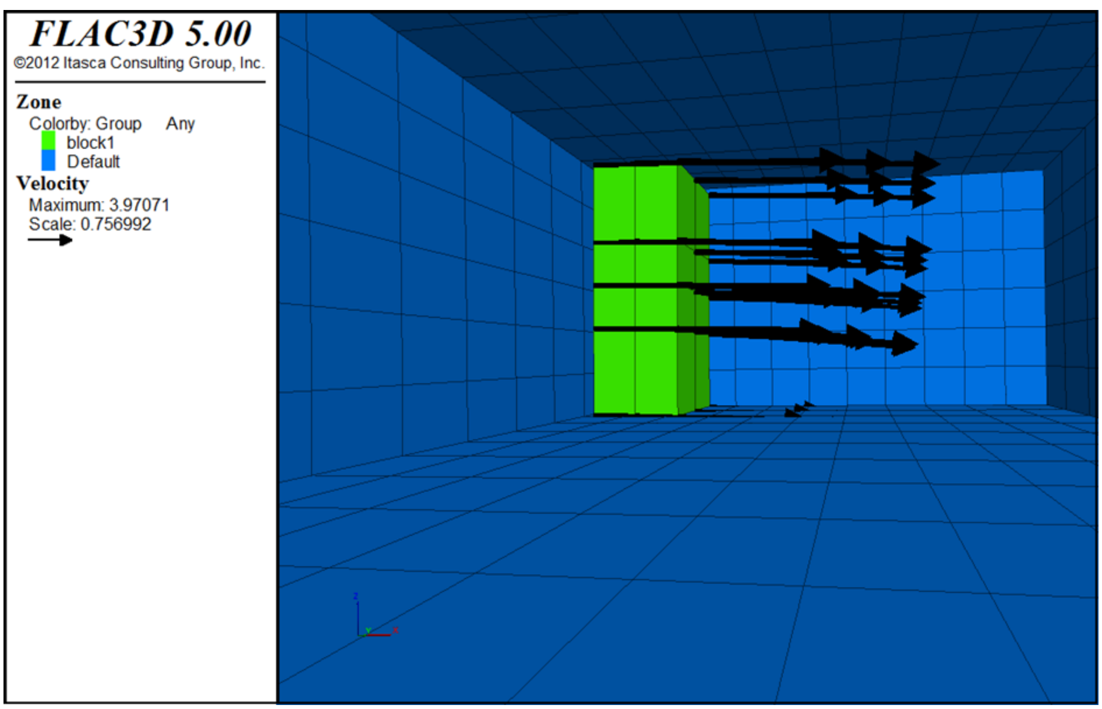

Figure 4 View inside of the excavated mine roadway showing the coal block ejection away from the rib side 0.07 seconds after the fault slip begun

Table 2 Modelled fault geometry, block ejection velocity and energy impacting on rib caused by fault slip

Fault No	Strike (°)	Dip (°)	Fault Distance from seam (m)	Block Ejection average velocity (m/s)	Block Momentum (mv) (kgm/s) x10^3	Energy impacting the rib 0.5mv^2 (Nm) x10^3
1	Parallel to seam	0°	20m Roof	4.1	17.1	35.8
2	Parallel to seam	0°	15m Roof	4.3	17.5	37.5
3	Parallel to seam	0°	10m Roof	4.4	17.9	39.3
4	Parallel to seam	0°	5m Roof	4.3	17.5	37.5
5	Parallel to seam	0°	2m Roof	3.5	14.2	24.9
6	Parallel to seam	0°	2m Floor	3.9	15.8	30.9
7	Parallel to seam	0°	5m Floor	4.5	18.3	41.1
8	Parallel to mining	0	10m Floor	4.6	18.7	43.0
9	Parallel to mining	0	15m Floor	4.6	18.7	43.0
10	Parallel to mining	0	20m Floor	4.5	18.3	41.1
11	Parallel to mining	15	20m Roof	4.1	16.6	34.1
12	Parallel to mining	15	15m Roof	4.3	17.5	37.5
13	Parallel to mining	15	10m Roof	4.3	17.5	37.5
14	Parallel to mining	15	5m Roof	4.4	17.9	39.3
15	Parallel to mining	15	2m Roof	4.3	17.5	37.5
16	Parallel to mining	15	2m Floor	4.3	17.5	37.5
17	Parallel to mining	15	5m Floor	4.6	18.7	43.0
18	Parallel to mining	15	10m Floor	4.4	17.9	39.3
19	Parallel to mining	15	15m Floor	4.7	19.1	44.8
20	Parallel to mining	15	20m Floor	4.2	17.1	35.8
21	Parallel to mining	30	20m Roof	4.0	16.2	32.5
22	Parallel to mining	30	15m Roof	4.5	18.3	41.1
23	Parallel to mining	30	10m Roof	4.4	17.9	39.3
24	Parallel to mining	30	5m Roof	4.2	17.1	35.8
25	Parallel to mining	30	2m Roof	4.2	17.1	35.8
26	Parallel to mining	30	2m Floor	4.2	17.1	35.8
27	Parallel to mining	30	5m Floor	4.2	17.1	35.8
28	Parallel to mining	30	10m Floor	4.3	17.5	37.5
29	Parallel to mining	30	15m Floor	4.3	17.5	37.5
30	Parallel to mining	30	20m Floor	4.2	17.1	35.8
31	Parallel to mining	45	15m Roof	4.2	17.1	35.8
32	Parallel to mining	45	10m Roof	4.4	17.9	39.3
33	Parallel to mining	45	5m Roof	4.4	17.9	39.3
34	Parallel to mining	45	2m Roof	4.4	17.9	39.3
35	Parallel to mining	45	2m Floor	4.2	17.1	35.8
36	Parallel to mining	45	5m Floor	4.2	17.1	35.8
37	Parallel to mining	45	10m Floor	4.2	17.1	35.8
38	Parallel to mining	45	15m Floor	4.2	17.1	35.8
39	Parallel to mining	60	10m Roof	3.7	15.0	27.8
40	Parallel to mining	60	5m Roof	3.6	14.6	26.3
41	Parallel to mining	60	2m Roof	3.6	14.6	26.3
42	Parallel to mining	60	2m Floor	3.0	12.2	18.3
43	Parallel to mining	60	5m Floor	3.0	12.2	18.3
44	Parallel to mining	60	10m Floor	2.8	11.4	15.9

Results from the additional vertical fault models are summarised in Table 3 at various inclinations parallel to the mine roadway.

Table 3 Modelled fault geometry, block ejection velocities and rib impact energy due to vertical fault slip ahead of the roadway face

Fault No	Strike (°) (0° perpendicular to roadway)	Dip (°)	Fault Distance ahead of roadway Face (m)	Block Ejection average velocity (m/s)	Block Momentum (*mv*) (kgm/s) x10^3	Energy impacting the rib $0.5mv^2$ (Nm) x10^3
45	0°	90°	3 m	4.9	19.9	48.7
46	0°	90°	6 m	4.9	19.9	48.7
47	0°	90°	9 m	4.9	19.9	48.7
48	0°	90°	12 m	5.0	20.3	50.8
49	0°	90°	15 m	5.0	20.3	50.8
50	15°	90°	3 m	4.9	19.9	48.7
51	15°	90°	6 m	4.9	19.9	48.7
52	15°	90°	9 m	4.9	19.9	48.7
53	15°	90°	12 m	5.0	20.3	50.8
54	15°	90°	15 m	4.8	19.5	46.8
55	30°	90°	3 m	4.5	18.3	41.1
56	30°	90°	6 m	4.5	18.3	41.1
57	30°	90°	9 m	4.6	18.7	43.0
58	30°	90°	12 m	4.6	18.7	43.0
59	30°	90°	15 m	4.4	17.9	39.3
60	45°	90°	3 m	3.8	15.4	29.3
61	45°	90°	6 m	3.8	15.4	29.3
62	45°	90°	9 m	3.8	15.4	29.3
63	45°	90°	12 m	3.8	15.4	29.3
64	45°	90°	15 m	3.8	15.4	29.3
65	60°	90°	3 m	2.7	11.0	14.8
66	60°	90°	6 m	2.7	11.0	14.8
67	60°	90°	9 m	2.8	11.4	15.9
68	60°	90°	12 m	2.8	11.4	15.9
69	60°	90°	15 m	2.8	11.4	15.9
70	-15°	90°	3 m	4.5	18.3	41.1
71	-15°	90°	6 m	4.6	18.7	43.0
72	-15°	90°	9 m	4.7	19.1	44.8
73	-15°	90°	12 m	4.6	18.7	43.0
74	-15°	90°	15 m	4.2	17.1	35.8
75	-30°	90°	3 m	4.2	17.1	35.8
76	-30°	90°	6 m	4.1	16.8	35.0
77	-30°	90°	9 m	4.0	16.2	32.5
78	-30°	90°	12 m	3.9	15.8	30.9
79	-30°	90°	15 m	3.8	15.4	29.3
80	-45°	90°	3 m	3.2	13.0	20.8
81	-45°	90°	6 m	3.2	13.0	20.8
82	-45°	90°	9 m	3.2	13.0	20.8
83	-45°	90°	12 m	3.2	13.0	20.8
84	-45°	90°	15 m	3.2	13.0	20.8
85	-60°	90°	3 m	2.5	10.2	12.7
86	-60°	90°	6 m	2.5	10.2	12.7
87	-60°	90°	9 m	2.5	10.2	12.7
88	-60°	90°	12 m	2.5	10.2	12.7
89	-60°	90°	15 m	2.5	10.2	12.7

DISCUSSIONS

The results summarised in Table 2 and 3 indicate that faults with the same slip characteristics at close proximity to the excavation appear to produce similar block ejection velocities. These velocities seem to be consistent with the maximum fault slip velocity V_p. This is not surprising. When tracing the velocities surrounding the nearby slipping fault, the peak particle velocities that spread through either the rock or softer coal have similar maximum velocities and directions to the slipping fault. This simplifies the understanding of basic seismic wave front propagation close to the slipping faults.

Observations of the coal block ejection indicated that the block parts located closer to the slipping fault experienced dynamic impact sooner causing block rotation and uneven ejection of these blocks.

Furthermore, fault inclination produced inclined impact to the rib, further affecting block ejection trajectories, causing the block to bounce up and down.

When observing a minor refraction of seismic waves at the rock/coal seam interface (due to a slower speed of seismic waves in softer coal), *PPV* concentrations within the seam were observed. An additional 45 dynamic fault models were performed on seams with various stiffnesses (results not tabulated here) which indicated a magnifying effect to the rib velocities of softer seams up to 19% more depending on the fault location and inclination.

Typically, fault slips generate seismic waves that quickly spread through the surrounding strata and impact the roadway rib side. The fault slip direction however impacts only one side of the roadway where the rib ejection is most likely to occur. If the fault location is known and direction of fault slip evaluated from ground stress, then the location of the possible rib ejection can be predicted.

The ability to predict the location of seismic impact can be very valuable for safety in coal mines. When mining through certain zones of fault influence, mine personnel can be advised to keep to the safer side of the roadway to minimise the possibility of potential harm.

CONCLUSIONS:

To study the fault induced seismic waves and its influence on coal bursts in 3-dimensions using $FLAC^{3D}$, 89 dynamic model instances comprising various fault slip locations and directions were simulated. The general behaviour of fault slip was discussed. When at close proximity to excavation, the fault slip behaves as an infinite slip plane with minimum energy dissipation. The modelled fault slip failure shows that this mechanism can generate a sufficient amount of seismic energy to produce a coal burst on its own. Fault slip can typically occur as the progressive excavations towards them gradually relieve the stress normal to the fault plane. The initial rib impact appears to be approximately proportional to the maximum velocity of fault slip. The fault slips release fast seismic waves with peak particle velocities (*PPV)* that can exceed several m/s. These models of different fault slip locations and orientations reveal fast ejections of the detached blocks in the roadway.

The results show that the coal burst typically occurs on one side of the roadway only in response to the approaching seismic waves. Once the location of the fault zone and direction of fault slip is estimated, the mine excavation side where probable rib ejection may occur, can be predicted. The models also show that the seismic waves tend to concentrate within the coal seam producing faster coal rib ejections. Overall, this research produced preliminary results to prove that this method can be used to flag the coal burst dangers for certain fault locations and orientations in deeper mines irrespective of the fault slip properties that are typically difficult to predict.

RECOMMENDATIONS

Further dynamic modelling of fault slips is desirable to refine the understanding of rib burst mechanisms that may lead to safer mining through faulted strata. These modelled results were conducted to prove the concept only and were not verified with measurements in underground mines as no reliable data were found within the timeframe of this project. It is suggested that further detailed studies be undertaken in future to verify these findings.

REFERENCES

Bizzarri A., (2012). Analytical representation of the faults slip velocity from spontaneous dynamic earthquake models. Journal of Geophysical Research, Solid Rock, Volume 117, Issue B6 June 2012.

Blake, W & Hedley, DGF 2003, Rockbursts: case studies from North American hard rock mines, Society for Mining, Metallurgy and Exploration, Englewood, pp. 121.

Nemcik,J.A., Venticinque G. (2019). Modelling of Dynamic Fracture Mechanisms For Improved Strata Control Design & Coal Burst Assessment. End of the project report ACARP C26054.

Ortlepp, W.D. (2000). Observation of mining-induced faults in an intact rock mass at depth. International Journal of Rock Mechanics and Mining Sciences 37(1):423-436

Gaetano Venticinque and Jan Nemcik, Numerical model of dynamic rock fracture process during coal burst, Proceedings of the 2020 Coal Operators' Conference, University of Wollongong - Mining Engineering, 12-14 February 2020, University of Wollongong, 275-280.

White, B.G. and J.K. Whyatt. 1999a. Differential wall rock movements associated with rock bursts, Lucky Friday Mine, Coeur d'Alene Mining District, Idaho, USA. In Rock Mechanics for Industry. Proceedings of the 37th U.S. Rock Mechanics Symposium, ed. by B. Amadei, R. L. Kranz, G. A. Scott, and P. H. Smeallie (Vail, CO, June 6-9, 1999). Rotterdam: Balkema, pp. 1051-1059.

White, B.G. and J.K. Whyatt. 1999b. Role of fault slip on mechanisms of rock burst damage, Lucky Friday Mine, Idaho, USA. In SARES 99: 2nd Southern African Rock Engineering Symposium. Implementing Rock Engineering Knowledge, T.O. Hagan, ed. (Johannesburg, S. Africa, Sept. 13-15, 1999). Johannesburg: Intern. Soc. Rock Mech., pp. 169-178.